

Study of the correlation between magnetic susceptibility and NMR relaxation using T₂-filtered and T₁-weighted CPMG

Everton Lucas-Oliveira^{a,*}, Marta Henriques Jácomo^b, Agide Gimenez Marassi^a,
Ricardo Ivan Ferreira da Trindade^c, Tito José Bonagamba^a

^a Sao Carlos Institute of Physics, University of Sao Paulo – IFSC/USP, Brazil

^b Institute of Geosciences, State University of Campinas – IG/UNICAMP, Brazil

^c Institute of Astronomy, Geophysics and Atmospheric Sciences, University of Sao Paulo – IAG/USP, Brazil

ARTICLE INFO

Keywords:

Relaxation time
Magnetic susceptibility
T₂-filtered CPMG
T₁-weighted CPMG

ABSTRACT

NMR is widely applied in Materials Science for the characterization of porous materials. The advantage of this technique is the high correlation between the NMR measurements and the physical-chemical features of the material. Magnetic susceptibility is one of many other properties that have been investigated by time domain NMR. In this work, the study of the influence of magnetic susceptibility on the relaxation process of micro and macroporosity is carried out, which is obtained using the T₂-filtered and T₁-weighted techniques combined with the CPMG experiment. This approach seeks to simplify the problem by treating microporosity and macro porosity conditions separately. The obtained data show the strong influence of the magnetic susceptibility on the relaxation times as expected, but showing more influence for the shorter ones, related to small pores.

1. Introduction

NMR is of great importance in the analysis of fluids in Porous Media, especially in the oil industry, where the NMR technique is applied both in the laboratory and for well-logging investigation (Dunn et al., 2002; George R. Coates, Lizhi Xiao, 1999). One of most important aspects of the NMR data obtained for the fluids in Porous Media is the relationship between the relaxation time and pore size, which allows obtaining information on micro and macroporosity. For example, for sandstones, the relaxation time distribution is divided into free fluid, irreducible water and clay bound water (Gonzalez et al., 2020).

Taking into account the relationship between NMR data and porous media features, much work has been done in the laboratory to investigate how other physical information can be accessed from relaxation time distribution, such as pore size, magnetic susceptibility, wettability and permeability. In general, this information is related to the morphology and mineralogical composition of the porous material (Howard, 1998; Jácomo et al., 2020; Lucas-Oliveira et al., 2021; Valori and Nicot, 2019).

Hürlimann (1998) developed a study about the effective magnetic field gradient that is generated inside porous due to magnetic susceptibility differences. He analyzed the magnetic field gradient using low

field NMR (2 MHz, for protons), and concluded that for carbonates the effective internal gradient field are typically smaller than gradient of NMR well logging tools, and for sandstones it can be comparable or larger.

Keating and Knight (2010), studied the effects of the magnetite concentration on NMR relaxation rates. However, no correlation trend was found between the magnetic susceptibility and relaxation rate. One of the explanations they offered to understand the lack of correlation was that the strong magnetic field gradient is localized and does not reflect in the relaxation rate.

In order to understand the magnetic susceptibility effects on NMR measurements and correlate them with bulk magnetic susceptibility, the relaxation time distributions can be obtained by controlling some parameters of NMR experiments (d'Eurydice et al., 2016; Hürlimann et al., 2002).

Sun and Dunn (2002) published a method where, through a modification of the CPMG method, it is possible to determine the distribution of the internal magnetic field gradient. Later, Xiao et al. (Xiao et al., 2013) added a dimension related to T₁ relaxation, allowing to combine T₁, T₂ and internal magnetic field. It should be noted that the method presented by Sun and Dunn is limited to pores associated with relaxation times greater than one fifth of the longest coding echo time.

* Corresponding author.

E-mail address: everton.lucas.oliveira@usp.br (E. Lucas-Oliveira).

The proposal of this work is to analyze whether micro and macro porosity are better related to magnetic susceptibility using relaxation filters before the CPMG pulse sequence (Carr and Purcell, 1954; Meiboom and Gill, 1958).

In this way, the relaxation time will be weighted by the total magnetization of the micro or macro porosity. Differently from what was proposed by Sun and Dunn, this work does not seek to determine the distribution of internal magnetic field gradients, but how the weight of T_1 and T_2 can influence the evolution of relaxation.

This study was performed for a set of 17 selected sandstones rocks, which magnetic susceptibilities ranging from 0.79×10^{-6} to 5.10×10^{-6} SI.

CPMG NMR experiments were performed using two strategies. One looking for longer relaxation times related to larger pores, and another to observe shorter relaxation times, which are associated with smaller pores. To observe longer relaxation times, T_2 -filtered technique (d'Eurydice et al., 2016) was used to suppress the short transverse relaxation times. To observe the signal weighted by the shortest transverse relaxation times, T_1 -weighted method was employed (Blümich et al., 1998).

1.1. Relaxation time on porous media

In general aspects, the NMR transverse relaxation time T_2 in Porous Media is well described in the literature (Dunn et al., 2002; Gonzalez et al., 2020) and can be related to three main contributions:

$$\frac{1}{T_2} = \frac{1}{T_2^S} + \frac{1}{T_2^D} + \frac{1}{T_2^B}, \quad (1)$$

where T_2^S is the relaxation time due to the interaction of the fluid molecules with the pore surface, T_2^D is the relaxation time due to the translational diffusion in the presence of magnetic field gradients, and T_2^B is the bulk relaxation time in the absence of other relaxation mechanisms than the interaction between the fluid molecules.

The T_2^S is described in detail by Brownstein and Tarr (1979). In the fast diffusion regime this relaxation time is proportional to the pore surface-to-volume ratio, given by:

$$\frac{1}{T_2^S} = \rho_2 \frac{S}{V}, \quad (2)$$

which shows that the T_2^S relaxation time has no direct dependence on NMR pulse sequence parameters. ρ_2 is the transverse surface relaxivity. Several works associate this parameter with the porous medium composition (Benavides et al., 2017; Gonzalez et al., 2020; Washburn et al., 2017). On the other hand, T_2^D relaxation time is related to the translational diffusion of the fluid molecules and, therefore, has a strong dependence on the echo time parameter t_e found in the CPMG pulse sequence. Considering a constant magnetic field gradient g , T_2^D can be written as:

$$\frac{1}{T_2^D} = \frac{D_0(\gamma g t_e)^2}{12} \quad (3)$$

In Eq. (3), D_0 is the bulk diffusion coefficient and γ is the nucleus gyromagnetic factor.

Hürlimann (1998) analyzed for both carbonates and sandstones the maximum magnitude of the internal magnetic field gradient in terms of the magnetic susceptibility difference of the fluid and porous materials $\Delta\chi$, establishing the following expression:

$$g_{max} \approx \left(\frac{\gamma}{D_0}\right)^{1/2} (\Delta\chi B_0)^{3/2}, \quad (4)$$

and, therefore, the relaxation time is expected to be proportional to the magnetic susceptibility difference $\Delta\chi$. B_0 is the static magnetic field

applied for the NMR experiments.

However, when the study is concentrated on a sample group saturated with a single fluid, the magnetic field gradient can be analyzed only as proportional to the bulk magnetic susceptibility of the rock matrix, since the fluid contribution would simply introduce a displacement relatively on the total magnetic susceptibility values.

Bearing in mind what was presented above about the relaxation in porous media and its dependence on internal magnetic field gradients, as well as the pore shape and mineralogical composition (Keating and Knight, 2012; Song, 2000), we proposed to study a set sandstone rocks with magnetic susceptibilities ranging from 0.79×10^{-6} to 5.10×10^{-6} SI, using two preparation methods preceding CPMG pulse sequence, Fig. 1a, which allow to observe, separately, short and long transverse relaxation times.

T_2 -filtered was used to suppress contributions from shorter relaxation times, in which a CPMG with fixed echo time (t_{echo}) and number of echoes (N_f) is applied. Thus, only components with relaxation times longer than $t_f = t_{echo}N_f$ still contribute to the total magnetization, which is measured by a second CPMG, Fig. 1b. The magnetization evolution during the second CPMG is given by,

$$M(t) = \sum m_i e^{-t/T_{2,i}} \quad (5)$$

where each m_i has already evolved during the first CPMG and can be written as:

$$m_i = m_{0,i} e^{-t_f/T_{2,i}}. \quad (6)$$

Here, $m_{0,i}$ is the total magnetization of each component of $T_{2,i}$. Therefore, the shorter the relaxation time $T_{2,i}$ of the m_i component, the lower it's the intensity for a fixed t_f .

On the other hand, the T_1 -weighted method was used to partially suppress longer longitudinal relaxation times, where a train of pulses is applied to saturate the magnetization previously to CPMG sequence. After saturation, the total magnetization is zero in any direction. Consequently, each magnetization component begins to recover under its corresponding T_1 relaxation, in which the components with short T_2 also have shorter T_1 , that is, returning faster to the z-direction. Therefore, after an evolution period of time t_w , which corresponds to the T_1 -weighting procedure (Blümich et al., 1998), a CPMG measurement is applied, and components with $T_1 \gg t_w$ will be suppressed, Fig. 1c. In this case, the magnetization evolution during the CPMG can be written by Eq. (5), but m_i is given by:

$$m_i = m_{0,i} (1 - e^{-t_w/T_{1,i}}) \quad (7)$$

where the shorter the longitudinal relaxation time $T_{1,i}$ of the m_i component, the greater its intensity m_i .

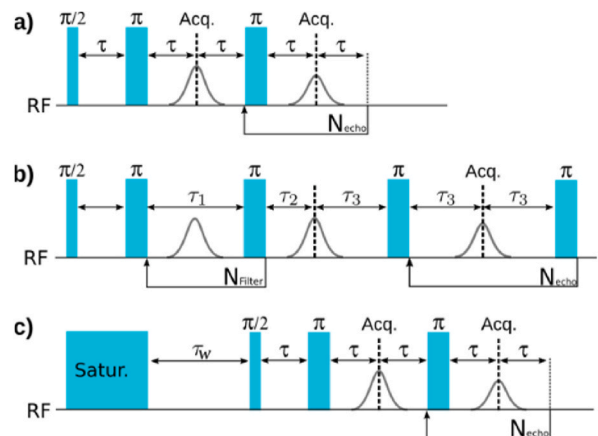


Fig. 1. NMR sequence for CPMG, T_2 -filtered CPMG and T_1 -weighted CPMG.

In general, the CPMG is used with short echo time to minimize the transverse relaxation time due to the translational diffusion effects in the presence of internal magnetic field gradients (Kleinberg and Horsfield, 1990). However, in order to evaluate the internal magnetic field gradients, the echo time is varied (Gonzalez et al., 2020). Thus, the relaxation time should be constant in the regime where the T_2^S dominates and vary linearly with echo time squared in the regime where T_2^D dominates. However, in complex porous media, T_2^D is related to both translational diffusion and internal magnetic field gradient (Gonzalez et al., 2020).

The proposal here is to analyze the dependence of the relaxation times on the echo time squared, calculating $f(g)$, in the region where the following relationship is linear:

$$\frac{1}{T_{2,LM}} = f(g)t_e^2 \tag{8}$$

where $T_{2,LM}$ is the log-mean of the transverse relaxation time obtained by CPMG, and $f(g) = \frac{D(\gamma g)^2}{12}$.

Another analysis performed was the measurement of the transverse relaxation times from the Hahn-Echo (Hahn, 1950), which is the first echo obtained in the CPMG sequence. Since the echo time of the CPMG sequence is varied, a curve of Hahn echoes is also obtained, which is known to be strongly influenced by the fluid molecules translational diffusion in the presence of an inhomogeneous magnetic field. Thus, a second relaxation time, $T_{2,Hahn}$, is obtained from the measurement of $m_1(t_e)$, the first echo on CPMG, for each sample.

2. Material and methods

This study was performed for a set of 17 selected sandstone rocks, whose bulk magnetic susceptibilities (χ_v) vary from 0.79×10^{-6} to 5.10×10^{-6} SI. They were indexed from A to P, in order of increasing bulk magnetic susceptibility (Table 1).

The magnetic susceptibility was also weighted by the porosity of each sample, in order to obtain the magnetic susceptibility χ_ϕ referring to the volume of the rock matrix instead of the total volume of the sample and these values will be used on the analyses.

The 1H 2 MHz NMR relaxation measurements were performed using two Tecmag components, a LapNMR console and a 0.047 T permanent magnet. The $\pi/2$ and π pulses were calibrated with durations of 13.6 μs and 27.2 μs , respectively. All measurements were performed using an averaging procedure with 32 scans. The recycling delay was set for each sample to be longer than $5T_1$. The echo times were adjusted from 150 to

Table 1
Porosity (ϕ), Volume magnetic susceptibility (χ_v), Porosity magnetic susceptibility (χ_ϕ) and estimated internal magnetic field gradients by the different methods.

Sample	Porosity ϕ	$\chi_v \times 10^{-6}$ SI	$\chi_\phi \times 10^{-6}$ SI	$g_{convent.}$ (G/cm)	g_{T_2} -filtered (G/cm)	g_{T_1} -weighted (G/cm)
A	0.15	0.79	0.67	130	160	170
B	0.22	0.77	0.60	70	60	120
C	0.22	0.89	0.68	90	80	130
D	0.26	0.84	0.63	90	80	130
E	0.14	1.02	0.87	260	190	220
F	0.14	1.12	0.97	350	270	200
G	0.17	1.18	0.98	250	200	220
H	0.21	1.57	1.24	140	120	170
I	0.18	1.74	1.43	200	180	190
J	0.23	1.90	1.46	310	230	250
K	0.15	2.06	1.76	370	300	270
L	0.20	2.30	1.84	270	190	300
M	0.23	2.52	1.94	610	460	400
N	0.14	2.18	1.89	320	340	300
O	0.15	2.60	2.22	600	550	500
P	0.08	5.10	4.68	750	400	560

2900 μs , using 10 logarithmically spaced values. All samples were saturated with distilled water, which in 25 °C has diffusion coefficient of $2.3 \times 10^{-9} m^2/s$.

Fig. 2, shows the relaxation decay for multiples echoes time for sample A to illustrate the magnetization decay that is obtained using different echo times. All decay curves have been shifted so that all CPMG first echoes are located at $t = 0$, since the evolution of magnetization after the first echo will be evaluated.

For each echo time, three CPMG signals were obtained for all samples: conventional, T_2 -filtered and T_1 -weighted. In the case of the T_2 -filtered CPMG experiments, they were performed using a filter defined by a train of 40 echoes spaced by 250 μs . For the T_1 -weighted experiments, they were performed with t_w of 100 ms.

Fig. 3 shows the transverse relaxation time distributions obtained for samples D and M using conventional, T_2 -filtered and T_1 -weighted CPMG experiments, with an echo time of 150 μs . While sample D, which has a wider T_2 distribution, is useful to demonstrate the effects of T_1 and T_2 filters, sample M contribute to observe the effect of the T_2 filter.

Using the same procedure presented for samples D and M, the transverse relaxation time distributions were obtained for all the samples. Afterwards, the $T_{2,LM}$ values were calculated for all the obtained T_2 distributions.

2.1. Magnetic susceptibility

Magnetic susceptibility can be defined as being the ability of mineral to be magnetized (Butler, 1992).

When the sample is subjected to a magnetic H field, it acquires an intensity of induced magnetization M_i , which is proportional to the applied field, given by, $M_i = \chi H$, where M_i is induced magnetization (A/m), χ is magnetic susceptibility (dimensionless in International System of Units or SI) and H is induced magnetic field (H) (A/m). Here, we used a MFK1-FA AGICO susceptometer operating at 976 Hz to measure the susceptibility of the samples. The values can be found on Table 1.

All the minerals present in the sample contribute to bulk χ . The difference of magnetic susceptibility between the fluid and the grain mineral surface induces a magnetic field gradient in the pore space, contributing to a faster $1/T_2$ relaxation rates (Keating and Knight, 2007). Zhang and Blümich (2015) showed a linear correlation between the internal magnetic field gradient and the magnetic susceptibility difference between fluid and solid. Since all samples are saturated with

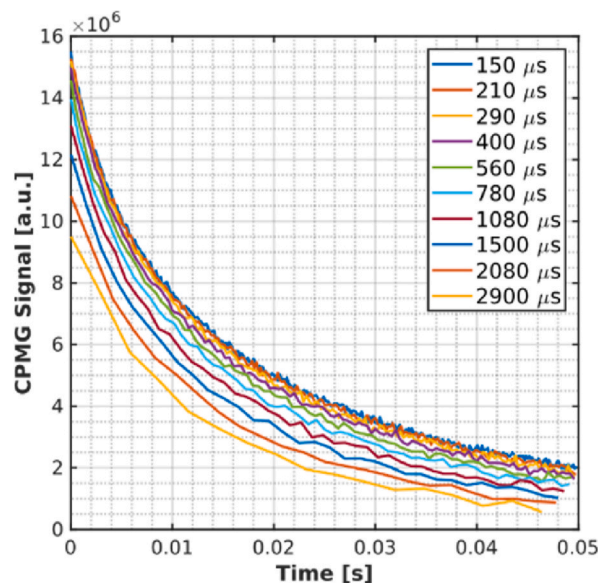


Fig. 2. CPMG decay for multiple echo times for sample A to illustrate the magnetization decay that is obtained using different echo time.

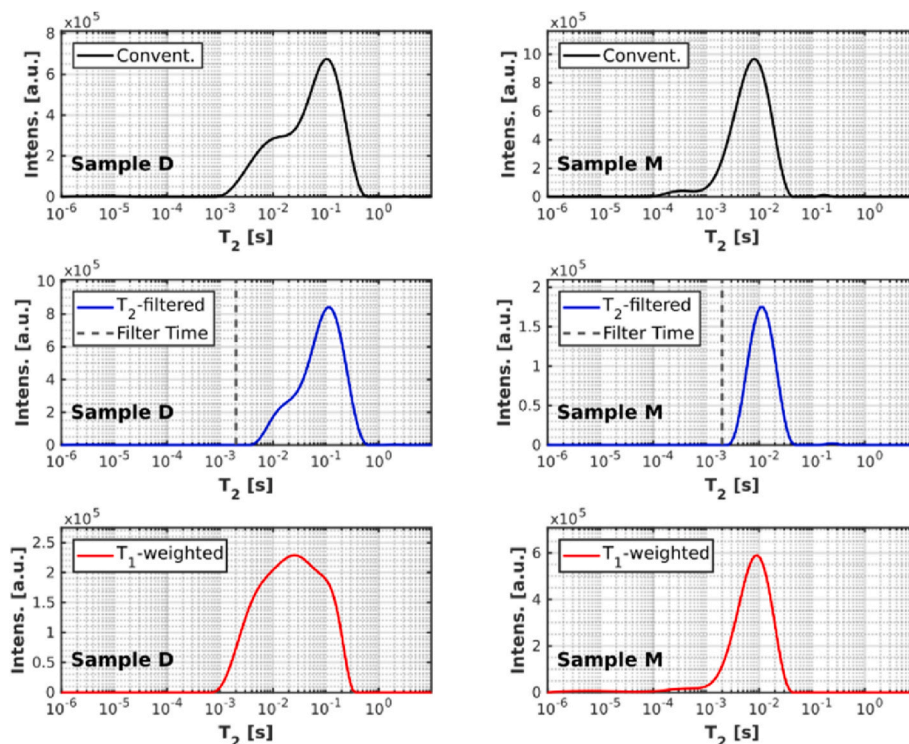


Fig. 3. Transverse relaxation time distributions obtained for samples D and M using conventional, T_2 -filtered and T_1 -weighted CPMG experiments, with an echo time of 150 μ s.

distilled water, the dye should be linear with the magnetic susceptibility of the porous medium as well.

3. Results and discussion

Fig. 4 shows the plots of $1/T_{2,LM}$ vs t_{echo}^2 obtained using the conventional CPMG method for all the samples, where one can observe a non-linear relationship (Fig. 4a). The linearity is expected in the regime where the magnetic field gradient can be approximated to a constant or average limit. It is also considered that the molecules have a free diffusion for the case of short echo times. A study of this non-linear behavior can be found in the work developed by Gonzales et al. (Gonzalez et al., 2020). Considering that for the first echoes the plot $1/T_{2,LM}$ vs t_{echo}^2 is closer to a linear relationship, the internal magnetic field gradient g was estimated considering the first five echo times (Fig. 4b), using Eq. (3).

Similar curves were obtained using T_2 -filtered and T_1 -weighted CPMG experiments. Using the value of the estimated $f(g)$, the internal magnetic field gradient g was calculate by Eq. (3) and summarized in Table 1.

Fig. 5 shows the plots of $f(g)$ obtained from conventional, T_2 -filtered and T_1 -weighted CPMG experiments vs the magnetic susceptibility χ_ϕ . All the three curves shown in Fig. 5 present similar trends, indicating a good correlation between $f(g)$ and magnetic susceptibility χ_ϕ . However, when comparing the measurements made with T_2 -filtered and T_1 -weighted CPMG experiments, the best correlation factor was found for the latter, $R^2 = 0.82$. In the case of T_2 -filtered CPMG, the correlation factor was $R^2 = 0.48$. Despite the difference in correlation factors, the gradient g shows the same order of magnitude when estimated by both filtering methods, Table 1.

Assuming that the transverse relaxation time is related to the pore size, Eq. (2), the higher correlation observed for shorter T_2 values seems

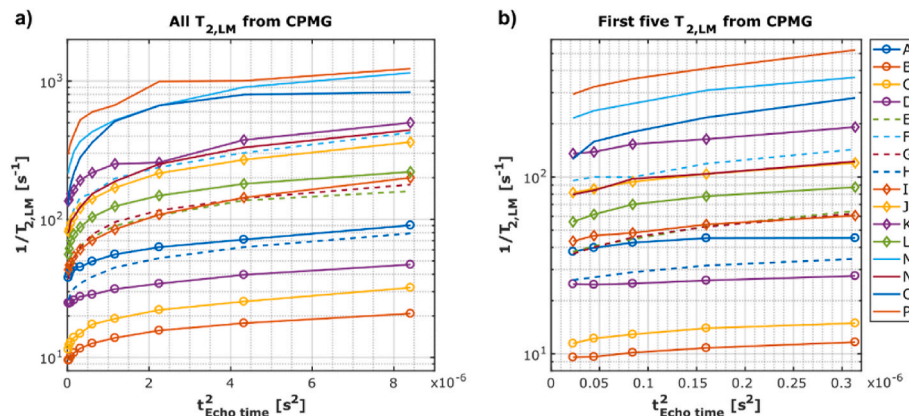


Fig. 4. Plots of $1/T_{2,LM}$ vs t_{echo}^2 obtained using the conventional CPMG method for all the samples and, plots of $1/T_{2,LM}$ vs t_{echo}^2 considering only the first five echo times.

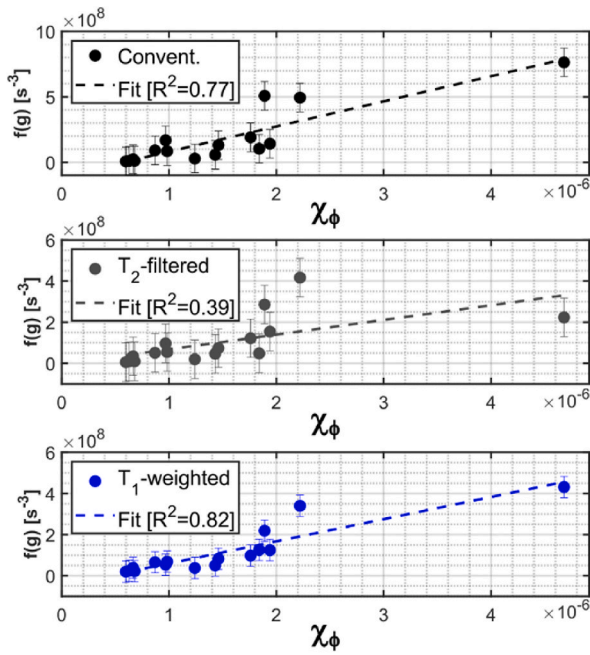


Fig. 5. Factor $f(g)$ vs. χ_ϕ . The factor f_g was estimated without filter, and using T_2 -filtered and T_1 -weighted.

to indicate that the fluid molecules occupying the smaller pores (micropores) are in a more intimate interaction with the gradient of the internal magnetic field. The fluid molecules in the smaller pores can be more affected because the internal magnetic field gradient is more intense in the micropores or the internal magnetic field gradient is higher mainly on the pore surface, consequently, the influence would be proportional to the surface-to-volume ratio of the pores.

As mentioned above, the Hahn-echo signal is also strongly influenced by the combination of the presence of inhomogeneous magnetic fields and fluid molecules diffusion.

Fig. 6 shows the Hahn-echo relaxation decays observed for all the samples, using conventional, T_2 -filtered and T_1 -weighted CPMG experiments. The observed decays already indicate an expressive variation in the relaxation times. However, it is not expected that only the magnetic susceptibility can explain this expressive distribution of relaxation times. Different pore morphologies, diffusive couplings and mineralogical compositions of the samples can also play a significant role.

The same processing was applied for the Hahn-Echo data and the obtained results are shown in Fig. 7. As previously observed for the

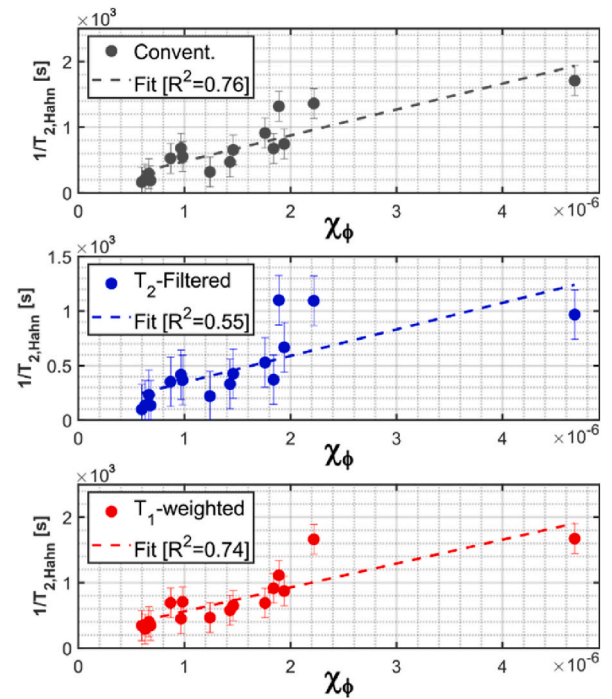


Fig. 7. Log-mean of the transverse relaxation rate measured by Hahn echo vs χ_ϕ , the last one with non-filter, T_2 -filtered and T_1 -weighted.

relaxation times obtained by multiple echoes, the T_1 -weighted presents a higher correlation factor, $R^2 = 0.74$, when compared with the T_2 -filtered, $R^2 = 0.55$.

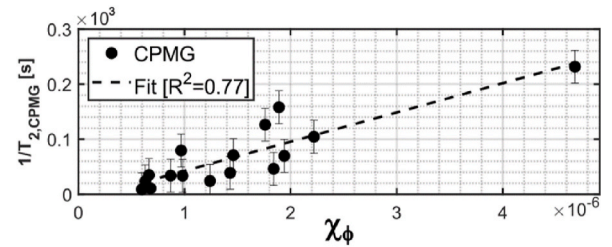


Fig. 8. Log-mean of the transverse relaxation rate measured by CPMG vs measured by Hahn echo, the last one with non-filter, T_2 -filtered and T_1 -weighted.

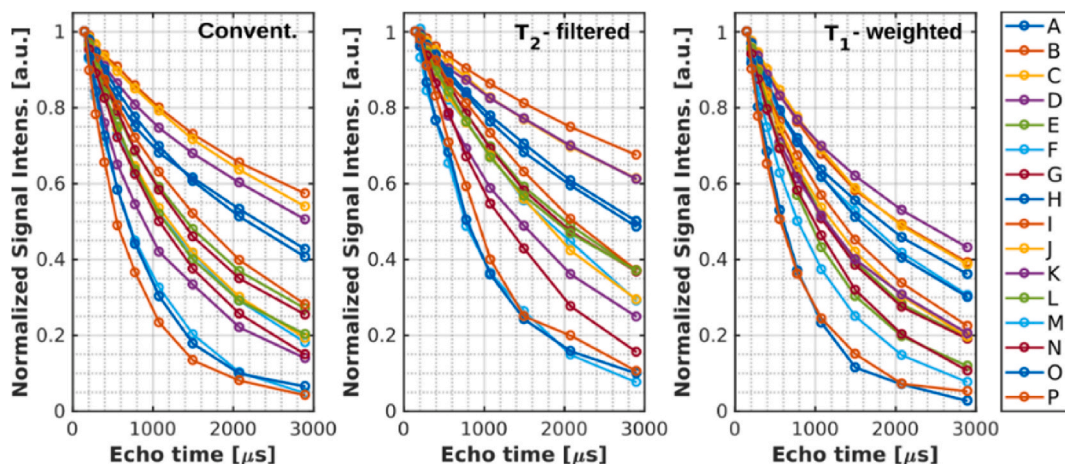


Fig. 6. Magnetization decay measured by Hahn echo for the 17 samples, with non-filter, T_2 -filtered and T_1 -weighted.

In addition to the proposed analyses, Fig. 8 shows the correlation ($R^2 = 0.77$) between the magnetic susceptibility and the $T_{2,LM}$ obtained by conventional CPMG. The echo time used was 150 μ s, which is the minimum for the experimental setup.

This indicates that for this set of samples, the $T_{2,LM}$ time have a tendency to be shorter the greater the susceptibility, even using a low magnetic field and short echo times. Taking into account that both the internal gradient and the surface relaxivity are proportional to the concentration of magnetic impurities and iron oxides in the studied rocks (Keating and Knight, 2012; Korb et al., 1998), it is not straightforward to conclude whether $T_{2,LM}$ is dominated by the term T_{2D} or T_{2S} under these conditions.

4. Conclusion

The data observed for this set of 17 sandstone samples showed the expected relation, where the greater the magnetic susceptibility, the greater the relaxation rate ($1/T_2^D$). However, even using low field NMR (2 MHz) and short echo time (150 μ s), the log-mean relaxation time obtained shows to be proportional to the magnetic susceptibility. This may indicate that the relaxation time is dominated by the surface relaxivity for this set of samples, which preserves the proportionality between relaxation time and pore size, but a wide range of surface relaxivity is expected. Thus, it is expected that in a future work, the pore size distribution can be obtained in order to estimate the surface relaxivity to directly analyze its correlation with susceptibility.

The pore size is an important parameter to also analyze the different correlation observed for the T_1 -weighted and the T_2 -filtered data. It was possible to observe that the variation of magnetization with echo spacing is greater for the fluid present in the microporosity than for the fluid present in the macro porosity. Thus, in addition to the pore size distribution, knowing the susceptibility present in micro and macro porosity can also contribute to increase the level of understanding of the observations highlighted in this work.

The method proposed by Sun and Dunn has some assumptions, such as the averaging limit that depends on diffusion time and pore scale. The method also limits the analysis to relaxation times longer than or of the same order as the echo time used in the first CPMG encoding. The data presented here showed a greater correlation between the magnetic susceptibility when weighted by the short relaxation time, and more efforts will be needed to evaluate the internal magnetic gradient field distribution for relaxation times of the order of a few milliseconds.

Credit author statement

All authors provided critical feedback and helped shape the research, analysis and manuscript. Everton Lucas-Oliveira: Conceptualization, Investigation, Validation, Methodology, Formal analysis, Writing-Original draft preparation and Editing. Marta Henirques Jácomo: Conceptualization, Methodology, Formal analysis, Writing-Original draft preparation. Writing-Reviewing and Editing. Agide Gimenez Marassi: Conceptualization, Investigation, Validation, Methodology, Formal analysis, Writing-Reviewing and Editing. Ricardo Ivan Ferreira da Trindade: Supervision, Conceptualization, Writing-Reviewing and Editing. Tito José Bonagamba: Supervision, Conceptualization, Writing-Original draft preparation. Writing-Reviewing and Editing.

Declaration of competing interest

The authors declare that they have no known competing financial interests or personal relationships that could have appeared to influence the work reported in this paper.

Data availability

Data will be made available on request.

Acknowledgements

Authors acknowledge the support of the following Brazilian Institutions: University of São Paulo (USP). T. J. Bonagamba acknowledges National Council for Scientific and Technological Development, Brazil (CNPq, 308076/2018–4) and São Paulo Research Foundation, Brazil (FAPESP, 2009/54880–6). Authors also acknowledge Eng. Edson L. G. Vidoto and Aparecido D. F. de Amorim for designing and assembling the NMR probes. The authors acknowledge also the National Agency of Petroleum, Natural Gas and Biofuels (ANP/Brazil) for support and providing the samples.

References

- Benavides, F., Leiderman, R., Souza, A., Carneiro, G., Bagueira, R., 2017. Estimating the surface relaxivity as a function of pore size from NMR T_2 distributions and microtomographic images. *Comput. Geosci.* 106, 200–208. <https://doi.org/10.1016/j.cageo.2017.06.016>.
- Blümich, B., Blümli, P., Eidmann, G., Guthausen, A., Haken, R., Schmitz, U., Saito, K., Zimmer, G., 1998. The NMR-MOUSE: construction, excitation, and applications. In: *Magnetic Resonance Imaging*, pp. 479–484. [https://doi.org/10.1016/S0730-725X\(98\)00069-1](https://doi.org/10.1016/S0730-725X(98)00069-1).
- Brownstein, K.R., Tarr, C.E., 1979. Importance of classical diffusion in NMR studies of water in biological cells. *Phys Rev A (Coll Park)* 19, 2446–2453. <https://doi.org/10.1103/PhysRevA.19.2446>.
- Butler, Robert F., 1992. *Paleomagnetism: magnetic domains to geologic terranes*. Blackwell Scientific Publications, Boston.
- Carr, H.Y., Purcell, E.M., 1954. Effects of diffusion on free precession in Nuclear Magnetic Resonance experiments. *Phys. Rev.* 94, 630–638. <https://doi.org/10.1103/PhysRev.94.630>.
- Coates, George R., Lizhi Xiao, M.G.P., 1999. *NMR Logging: Principles and Applications*. Halliburton Energy Services, Houston.
- Dunn, K.-J., Bergman, D.J., Latorraca, G.A., 2002. *Nuclear Magnetic Resonance: Petrophysical and Logging Applications*. Pergamon, San Ramon.
- d'Eurydice, M.N., Montrazi, E.T., Fortulan, C.A., Bonagamba, T.J., 2016. T_2 -filtered T_2 - T_2 exchange NMR. *J. Chem. Phys.* 144, 204201 <https://doi.org/10.1063/1.4951712>.
- Gonzalez, J.L., de Faria, E.L., Albuquerque, Marcelo P., Albuquerque, Marcio P., Bom, C. R., Freitas, J.C.C., Correia, M.D., 2020. Simulations of NMR relaxation in a real porous structure: pre-asymptotic behavior to the localization regime. *Appl. Magn. Reson.* 51, 581–595. <https://doi.org/10.1007/s00723-020-01200-6>.
- Hahn, E.L., 1950. Spin echoes. *Phys. Rev.* 80, 580–594. <https://doi.org/10.1103/PhysRev.80.580>.
- Howard, J.J., 1998. Quantitative estimates of porous media wettability from proton NMR measurements. *Magn. Reson. Imaging* 16, 529–533. [https://doi.org/10.1016/S0730-725X\(98\)00060-5](https://doi.org/10.1016/S0730-725X(98)00060-5).
- Hürlimann, M.D., 1998. Effective gradients in porous media due to susceptibility differences. *J. Magn. Reson.* 131, 232–240. <https://doi.org/10.1006/JMRE.1998.1364>.
- Hürlimann, M.D., Venkataramanan, L., Flaum, C., Speier, P., Karmonik, C., Freedman, R., Heaton, N., 2002. Diffusion-editing: new NMR measurement of saturation and pore geometry. In: *SPWLA 43rd Annual Logging Symposium 2002*. In: <https://onepetro.org/SPWLAALS/proceedings-abstract/SPWLA-2002/Ail-SPWLA-2002/SPWLA-2002-FFF/27448>.
- Jácomo, M.H., Trindade, R.I.F., Lucas-Oliveira, E., Bonagamba, T.J., 2020. Magnetic matrix effects on NMR relaxation times in sandstones: a case study in Solimões Basin. *J. Appl. Geophys.* 179 <https://doi.org/10.1016/j.jappgeo.2020.104081>.
- Keating, K., Knight, R., 2007. A laboratory study to determine the effect of iron oxides on proton NMR measurements. *Geophysics* 72 (1), E27–E32. <https://doi.org/10.1190/1.2399445>.
- Keating, K., Knight, R., 2010. A laboratory study of the effect of Fe(II)-bearing minerals on nuclear magnetic resonance (NMR) relaxation measurements. *Geophysics* 75, F71–F82. <https://doi.org/10.1190/1.3386573>.
- Keating, K., Knight, R., 2012. The effect of spatial variation in surface relaxivity on nuclear magnetic resonance relaxation rates. *Geophysics* 77, E365–E377. <https://doi.org/10.1190/geo2011-0462.1>.
- Kleinberg, R.L., Horsfield, M.A., 1990. Transverse relaxation processes in porous sedimentary rock. *J. Magn. Reson.* 88 (1969), 9–19. [https://doi.org/10.1016/0022-2364\(90\)90104-H](https://doi.org/10.1016/0022-2364(90)90104-H).
- Korb, J.-P., Whaley-Hodges, M., Bryant, R.G., 1998. Translational diffusion of liquids at surfaces of microporous materials: theoretical analysis of field-cycling magnetic relaxation measurements. *Magn. Reson. Imaging* 16, 575–578. [https://doi.org/10.1016/S0730-725X\(98\)00051-4](https://doi.org/10.1016/S0730-725X(98)00051-4).
- Lucas-Oliveira, E., Araújo-Ferreira, A.G., Bonagamba, T.J., 2021. Surface relaxivity probed by short-diffusion time NMR and Digital Rock NMR simulation. *J. Pet. Sci. Eng.* 207 <https://doi.org/10.1016/j.petrol.2021.109078>.

- Meiboom, S., Gill, D., 1958. Modified spin-echo method for measuring nuclear relaxation times. *Rev. Sci. Instrum.* 29, 688–691. <https://doi.org/10.1063/1.1716296>.
- Song, Y.-Q., 2000. Determining pore sizes using an internal magnetic field. *J. Magn. Reson.* 143, 397–401. <https://doi.org/10.1006/JMRE.1999.2012>.
- Sun, B., Dunn, K.J., 2002. Probing the internal field gradients of porous media. *Phys. Rev. E* 65, 051309. <https://doi.org/10.1103/PhysRevE.65.051309>.
- Valori, A., Nicot, B., 2019. A review of 60 Years of NMR wettability. *Petrophysics - The SPWLA Journal of Formation Evaluation and Reservoir Description* 60, 255–263. <https://doi.org/10.30632/PJV60N2-2019A3>.
- Washburn, K.E., Sandor, M., Cheng, Y., 2017. Evaluation of sandstone surface relaxivity using laser-induced breakdown spectroscopy. *J. Magn. Reson.* <https://doi.org/10.1016/j.jmr.2016.12.004>.
- Xiao, L., Liu, H., Deng, F., Zhang, Z., An, T., Zong, F., Anferov, V., Anferova, S., 2013. Probing internal gradients dependence in sandstones with multi-dimensional NMR. *Microporous Mesoporous Mater.* 178, 90–93. <https://doi.org/10.1016/J.MICROMESO.2013.04.003>.
- Zhang, Y., Blümich, B., 2015. Gint2D-T2 correlation NMR of porous media. *J. Magn. Reson.* 252, 176–186. <https://doi.org/10.1016/J.JMR.2015.01.009>.